0026-895X/10/7705-804–817$20.00
MOLECULAR PHARMACOLOGY
Vol. 77, No. 5
62208/3581477
Mol Pharmacol 77:804–817, 2010
Printed in U.S.A.

Modulation of Silent and Constitutively Active Nociceptin/Orphanin FQ Receptors by Potent Receptor Antagonists and Na^+ Ions in Rat Sympathetic Neurons

Saifeldin Mahmoud, Wojciech Margas, Claudio Trapella, Girolamo Caló, and Victor Ruiz-Velasco

Department of Anesthesiology, Penn State College of Medicine, Hershey, Pennsylvania (S.M., W.M., V.R.-V.); Department of Experimental and Clinical Medicine, Section of Pharmacology, and Neuroscience Center (G.C.), and Department of Pharmaceutical Science (C.T.), University of Ferrara, Ferrara, Italy

Received November 6, 2009; accepted February 16, 2010

ABSTRACT

The pharmacology of G protein-coupled receptors can be influenced by factors such as constitutive receptor activation and Na^+ ions. In this study, we examined the coupling of natively and heterologously expressed nociceptin/orphanin FQ (N/OFQ) peptide (NOP) receptors with voltage-dependent Ca^{2+} channels after exposure to four high-affinity NOP receptor blockers [[Nphe^{1}Arg^{14}Lys^{15}]N/OFQ-NH_2 (UFP-101), 1-[1-(cyclooctylmethyl)-1,2,3,6-tetrahydro-5-(hydroxymethyl)-4-pyridinyl]-3-ethyl-1,3-dihydro-2*H*-benzimidazol-2-one (Trap-101), 1-benzyl-*N*-{3-[spiroisobenzofuran-1(3*H*),4′-piperidin-1-yl]propyl}pyrrolidine-2-carboxamide (compound 24), and *N*-(4-amino-2-methylquinolin-6-yl)-2-(4-ethylphenoxymethyl)benzamide hydrochloride (JTC-801)] in sympathetic neurons. The enhanced tonic inhibition of Ca^{2+} currents in the absence of agonists, indicative of constitutively active NOP receptors in transfected neurons, was abolished after pretreatment with pertussis toxin. In control neurons, the four antagonists did not exert any effects when applied alone but significantly blocked the N/OFQ-mediated Ca^{2+} current inhibition. Exposure of transfected neurons to UFP-101 resulted in partial agonist effects. In contrast, Trap-101, compound 24, and JTC-801 exerted inverse agonism, as measured by the loss of tonic Ca^{2+} current inhibition. In experiments designed to measure the N/OFQ concentration-response relationship under varying Na^+ concentrations, a leftward shift of IC_{50} values was observed after Na^+ exposure. Although similar N/OFQ efficacies were measured with all solutions, a significant decrease of Hill coefficient values was obtained with increasing Na^+ concentrations. Examination of the allosteric effects of Na^+ on heterologously overexpressed NOP receptors showed that the tonic Ca^{2+} current inhibition was abolished in the presence of the monovalent cation. These results demonstrate that constitutively active NOP receptors exhibit differential blocker pharmacology and allosteric regulation by Na^+. Data are also presented demonstrating that heterologously expressed μ opioid receptors in sympathetic neurons are similarly modulated.

G protein-coupled receptors (GPCRs) make up the largest family of cell surface receptors that transduce signals across the cell membrane via the heterotrimeric G$\alpha\beta\gamma$ proteins. Once GPCRs are activated by ligands, Gα and G$\beta\gamma$ protein subunits, in turn, act on their effectors, such as ion channels (e.g., Ca^{2+} channels) and enzymes (e.g., adenylyl cyclases), to initiate a cellular response. Some GPCRs, however, have been shown to spontaneously activate in the absence of agonists. The constitutively active conformation of GPCR can be naturally occurring, virally induced, genetically engineered, and heterologously overexpressed in several cell systems (de Ligt et al., 2000; Seifert and Wenzel-Seifert, 2002). With heterologous overexpression, the high levels of receptors will spontaneously adopt an active state (de Ligt et al., 2000;

This work was supported by the National Institutes of Health National Institute on Drug Abuse [Grant R01-DA025574] and Tobacco Settlement Funds from the Pennsylvania Department of Health.
Article, publication date, and citation information can be found at http://molpharm.aspetjournals.org.
doi:10.1124/mol.109.062208.

ABBREVIATIONS: GPCR, G protein-coupled receptor; NOP, nociceptin/orphanin FQ peptide; N/OFQ, nociceptin/orphanin FQ; SG, stellate ganglion; MOP, μ opioid peptide; Trap-101, 1-[1-(cyclooctylmethyl)-1,2,3,6-tetrahydro-5-(hydroxymethyl)-4-pyridinyl]-3-ethyl-1,3-dihydro-2*H*-benzimidazol-2-one; compound 24, 1-benzyl-*N*-{3-[spiroisobenzofuran-1(3*H*),4′-piperidin-1-yl]propyl}pyrrolidine-2-carboxamide; UFP-101, [Nphe^{1}Arg^{14}Lys^{15}]N/OFQ-NH_2; JTC-801, *N*-(4-amino-2-methylquinolin-6-yl)-2-(4-ethylphenoxymethyl)benzamide hydrochloride; PTX, pertussis toxin; DAMGO, [D-Ala^2-*N*-Me-Phe^4-Glycol^5]-enkephalin; CTAP, D-Phe-Cys-Tyr-D-Trp-Arg-Thr-Pen-Thr-NH_2; NMG, *N*-methyl-D-glucamine; TEA-OH, tetraethylammonium hydroxide; J-113397, (±)-1-[(3*R**,4*R**)-1-(cyclooctylmethyl)-3-(hydroxymethyl)-4-piperidinyl]-3-ethyl-1,3-dihydro-2*H*-benzimidazol-2-one.

Seifert and Wenzel-Seifert, 2002; Strange, 2002). The active conformation of the receptors can be observed and measured, including an increase in tonic activity of receptor effectors.

The two most common pharmacological tools used to study constitutively active GPCRs are inverse agonists and Na^+ ions (Seifert and Wenzel-Seifert, 2002). Inverse agonists are compounds that are considered neutral antagonists with no known intrinsic activity but can inhibit constitutively active GPCR. Furthermore, these ligands can exhibit full or partial inverse agonist activity. The first report of inverse agonism in GPCRs was shown to occur with the δ opioid peptide receptor blockers (Costa and Herz, 1989). Several drugs known to be antagonists have been reported to be inverse agonists (Strange, 2002; Milligan and Smith, 2007). The exact mechanism by which inverse agonists achieve their effect is not entirely clear. With regard to Na^+ effects on constitutively active GPCRs, it is believed that the cation stabilizes the receptors into the "resting" state and thus behaves as an allosteric inverse agonist (de Ligt et al., 2000; Seifert and Wenzel-Seifert, 2002; Strange, 2002). The Na^+-mediated modulation of constitutively active GPCRs was initially demonstrated in δ opioid peptide receptors natively expressed in NG108-15 (Costa et al., 1990). It was shown that the presence of NaCl decreased the binding of opioid agonists. Subsequently, the allosteric effects mediated by Na^+ have been shown in several GPCR expression systems (Seifert and Wenzel-Seifert, 2002), including the nociceptin/orphanin FQ (N/OFQ) peptide (NOP) receptor (Ardati et al., 1997; Butour et al., 1997; Dooley and Houghten, 2000).

The NOP receptor was identified as an opioid receptor-like receptor (Mogil and Pasternak, 2001; Lambert, 2008) whose endogenous ligand is the 17-amino acid peptide N/OFQ (Meunier et al., 1995; Reinscheid et al., 1995). It has been shown recently that high expression levels of NOP receptors in tsa-201 cells exhibited tonic activation and formed a complex with N-type Ca^{2+} channels in the absence of agonists (Beedle et al., 2004). The agonist-independent modulation of Ca^{2+} currents was a result of the physical interaction between constitutively active receptors and the channel's C terminus (Beedle et al., 2004). Furthermore, Lambert and colleagues (McDonald et al., 2003; Barnes et al., 2007) have used the Chinese hamster ovary cell line to control NOP receptor expression levels ("pseudophysiological" and "supraphysiological") with an ecdysone-inducible system. They reported that the pharmacological profile of NOP receptor partial agonists depends on receptor expression levels, such that the compounds can behave as pure antagonists (low receptor expression levels) or as partial or even full agonists (intermediate or high receptor expression levels). In addition, upregulation of N/OFQ or NOP receptor mRNA and/or protein levels has been demonstrated in animal pain models, such as peripheral inflammation (Andoh et al., 1997; Jia et al., 1998), allodynia (Briscini et al., 2002), and neuropathy (Mika et al., 2004). Finally, a clinical study found that N/OFQ plasma levels were significantly elevated in patients with either acute or chronic pain compared with normal healthy volunteers (Ko et al., 2002).

We reported previously that the N/OFQ-mediated activation of natively expressed NOP receptors in rat stellate ganglion (SG) neurons results in voltage-dependent inhibition of Ca^{2+} channels (Ruiz-Velasco et al., 2005). In the present study, we examined whether NOP receptor overexpression in SG neurons would result in tonic receptor activation. Constitutive activation of NOP receptors in transfected neurons would result in tonic Ca^{2+} channel inhibition as measured with the whole-cell patch-clamp technique. The pharmacological profiles of four high-affinity NOP receptor blockers [UFP-101, Trap-101, compound 24, and JTC-801] were then measured to determine whether they would exhibit a different pharmacological activity under conditions in which the receptors are constitutively active. In addition, we examined the effect of Na^+ ions on the N/OFQ-mediated Ca^{2+} current inhibition and whether the constitutively active receptors are modulated by this cation.

Materials and Methods

SG Neuron Isolation. All experiments that used animal research were approved by the Penn State College of Medicine Institutional Animal Care and Use Committee. SG neurons were isolated from adult rats using the method described previously (Margas et al., 2008). In brief, male Wistar rats (125–175 g) were first anesthetized with CO_2 and then decapitated with a laboratory guillotine. Thereafter, the SG was cleared of connective tissue in ice-cold Hanks' balanced salt solution (Sigma-Aldrich, St. Louis, MO). The ganglia were enzymatically dissociated in a modified Earle's balanced salt solution containing 0.6 mg/ml collagenase (Roche Pharmaceuticals, Basel, Switzerland) and 0.4 mg/ml trypsin (Worthington Biochemical, Lakewood, NJ) in a shaking water bath at 35°C for 60 min. The neurons were then dispersed by vigorous shaking, centrifuged twice for 6 min at 63*g*, and resuspended in minimal essential medium, supplemented with 10% fetal calf serum, 1% glutamine, and 1% penicillin-streptomycin (all from Invitrogen, Carlsbad, CA). The dissociated neurons were then plated onto 35-mm poly(L-lysine)-coated dishes and stored in a humidified incubator (5% CO_2/95% air) at 37°C.

Microinjection of cDNA Plasmids. Microinjection of cDNA plasmids was performed 3 to 5 h after plating the neurons with an Eppendorf 5246 microinjector and 5171 micromanipulator (Eppendorf North America, New York, NY) as described previously (Ikeda, 2004). The plasmid coding for rat NOP receptor was subcloned in pCI and injected at a final concentration of 100 to 800 ng/μl. We isolated and cloned this receptor construct previously from SG neurons and found that adult rats express a single NOP receptor subtype or one splice variant (Ruiz-Velasco et al., 2005). The plasmid coding for the human μ opioid peptide (MOP) receptor was subcloned in pcDNA3.1 (Invitrogen) and injected at a concentration of 500 ng/μl. The "enhanced" green fluorescent protein (Clontech, Mountain View, CA) cDNA was coinjected at 5 ng/μl to allow for the identification of successfully injected neurons.

Electrophysiology and Data Analysis. Whole-cell Ca^{2+} currents were recorded using the patch-clamp technique. Electrophysiological recordings of all neurons were initiated within 24 h after intramuscular microinjection of plasmids to avoid neuronal process formation that would interfere with obtaining proper space clamp. Under these conditions, the mean (± S.E.) Ca^{2+} current density in control and transfected neurons was 36.8 ± 2.0 (n = 66) and 33.4 ± 2.1 (n = 56), respectively (P = 0.28). Thus, cDNA microinjection did not overtly affect Ca^{2+} channel currents. The patch pipette electrodes, fabricated from borosilicate glass (Garner Glass Co., Claremont, CA), were pulled on a P-97 micropipette puller (Sutter Instrument Co., Novato, CA). Ca^{2+} currents were acquired with the Axopatch 200B amplifier (Molecular Devices, Sunnyvale, CA), analog filtered at frequency 2 kHz (−3 dB, four-pole low-pass Bessel filter), and digitized with custom-designed S5 software (Stephen R. Ikeda, National Institute on Alcohol Abuse and Alcoholism, National Institutes of Health, Bethesda, MD) equipped with an 18-bit AD converter board (Intrudes Corp., Elmont, NY). Cell membrane ca-

pacitance and pipette series resistance were electronically compensated (80–85%).

Ca^{2+} currents were evoked with the double-pulse voltage protocol (Ikeda, 1991) shown in Fig. 1A (right). This protocol has been used routinely to study the agonist-mediated voltage-dependent inhibition of Ca^{2+} channel currents, including N/OFQ (Ruiz-Velasco et al., 2005). The protocol consists of a test pulse to +10 mV (prepulse, ●) followed by a large depolarizing conditioning test pulse to +80 mV, a brief return to −80 mV, and followed by a test pulse to +10 mV (postpulse, ○). The peak Ca^{2+} current amplitude was measured isochronally 10 ms after the initiation of the prepulse and postpulse. The agonist-mediated Ca^{2+} current inhibition (or enhancement) was calculated as follows: [peak Ca^{2+} current (prepulse before agonist) − peak Ca^{2+} current (prepulse after agonist)]/[peak Ca^{2+} current (prepulse before agonist)] × 100. Facilitation ratio was determined by dividing the postpulse by the prepulse current amplitude. In the absence of agonists, the facilitation ratio typically ranges between 1.1 and 1.3. On the other hand, the ratio generally reaches values between 1.5 and 4.0 when agonists are applied. Accordingly, in transfected SG neurons, the criterion used to define tonic inhibition of the Ca^{2+} currents in the absence of agonist was a facilitation ratio greater than 1.50.

Data and statistical analyses were performed with Igor Pro 6.0 (Lake Oswego, OR) and Prism 4.0 (GraphPad Software, Inc., San Diego, CA) software packages with $P < 0.05$ considered statistically significant. Graphs and current traces were generated with Igor Pro and Canvas 8.0 (Deneba Software, Miami, FL) software packages. The N/OFQ concentration-response relationships were determined by the sequential application of the receptor agonist in increasing concentrations. Two to three different concentrations were used with each neuron to minimize desensitization. The results were then pooled, and the concentration-response curves were fit to the Hill equation: $I = I_{max}/\{1 + (IC_{50}/[ligand])^{n_H}\}$, where I is the percentage inhibition, I_{max} is the maximum inhibition of the Ca^{2+} current, IC_{50} is the half-inhibition concentration, [ligand] is the agonist concentration, and n_H is the Hill coefficient. These parameters were obtained with Prism 4.0 software (GraphPad Software). All data are presented as mean ± S.E.

Solutions and Drugs. The external solution, referred to in the text as "TEA external," contained 145 mM tetraethylammonium hydroxide (TEA-OH), 140 mM methanesulfonic acid, 10 mM HEPES, 15 mM glucose, 10 mM $CaCl_2$, and 0.0003 mM tetrodotoxin, pH 7.40 with TEA-OH, and an osmolality of 316 to 321 mOsm/kg. In later experiments, we used three external solutions that contained 120, 60, and 12 mM Na^+ and are referred to as "120 Na^+ external," "60 Na^+ external," and "12 Na^+ external," respectively. The "120 Na^+ external" contained 120 mM $NaMeSO_3$, 35 mM TEA-OH, 10 mM HEPES, 10 mM $CaCl_2$, 10 mM glucose, and 0.0003 mM tetrodotoxin, pH 7.40 with TEA-OH, and an osmolality of 316 to 321 mOsm/kg. For both 60 and 12 mM Na^+ external solutions, the Na^+ concentration was lowered, and the appropriate amount of TEA-OH was added to keep the osmolality constant. The pipette internal solution, referred to as "NMG internal" contained 120 mM *N*-methyl-D-glucamine (NMG) 120, 20 mM TEA-OH, 20 mM HCl, 11 mM EGTA, 10 mM HEPES, 1 mM $CaCl_2$, 4 mM MgATP, 0.3 mM Na_2GTP, and 14 mM Tris-creatine phosphate, pH 7.20, and an osmolality of 305 mOsm/kg. In experiments in which Na^+ external solutions were used, the internal solution ("Cs^+ internal") contained 90 mM NMG, 25 mM TEA-OH, 11 mM EGTA, 10 mM HEPES, 1 mM $CaCl_2$, 20 mM CsCl, 20 mM CsOH, 4 mM MgATP, 0.3 mM Na_2GTP, and 14 mM Tris-creatine phosphate, pH 7.2, and an osmolality of 306 mOsm/kg. The recordings described for Figs. 1 to 4 were performed in TEA external and NMG internal solutions.

Stock solutions of N/OFQ, UFP-101 (both from Tocris Cookson, Ellisville, MO), [D-Ala^2-*N*-Me-Phe^4-$Glycol^5$]-enkephalin (DAMGO), D-Phe-Cys-Tyr-D-Trp-Arg-Thr-Pen-Thr-NH_2 (CTAP) (both from Sigma-Aldrich) and ω-conotoxin GVIA (Bachem, Torrance, CA) were prepared in H_2O, whereas stock solutions for Trap-101, compound 24, and JTC-801 were prepared in dimethyl sulfoxide. JTC-801 was from Tocris Cookson, whereas Trap-101 and compound 24 were prepared in house as described previously (Trapella et al., 2006, 2009). All agents were diluted in the external solution to their final concentration before use. In experiments in which the lipid-soluble NOP receptor blockers were used, an equivalent amount of dimethyl sulfoxide (0.01%) was added to the control external solution. Drugs were applied to the neuron under study with a custom-designed gravity-fed perfusion system that was positioned approximately 100 mm from the cell. The line delivering the external solution with no drugs was kept continuously open until the desired solution containing drugs or different Na^+ ion concentrations was used. Pertussis toxin (PTX; List Biological Laboratories, Inc., Campbell, CA) was prepared in water and added to the culture medium (12–20 h) at a final concentration of 500 ng/ml.

Results

UFP-101 Displays Partial Agonist Activity in SG Neurons Overexpressing NOP Receptors. The present study examined the pharmacology of constitutively active NOP receptors by high-affinity receptor blockers and Na^+ ions in acutely isolated rat SG neurons. Tonic activation of NOP receptors was attained by heterologously overexpressing the receptors in SG neurons. Figure 1A shows the time course of Ca^{2+} currents from a control SG neuron that were evoked every 10 s with the double-pulse protocol (described under *Materials and Methods*). Before application of the NOP receptor agonist N/OFQ, the activation phase of the prepulse (Fig. 1A, trace 1, right) was fast and reached a plateau approximately 5 to 10 ms after the onset of the pulse. On the other hand, exposure to N/OFQ (0.1 μM) led to a block of the prepulse current and to the kinetic slowing of the prepulse rising phase (Fig. 1A, trace 3, right). The kinetic slowing is believed to result from a voltage-dependent relief of block during the test pulse. Furthermore, the facilitation of Ca^{2+} currents can be observed by comparing the prepulse and postpulse current amplitudes of the superimposed traces shown (traces 1–4). Before N/OFQ application, the conditioning pulse to +80 mV had a minor effect on the postpulse current amplitude (compare Fig. 1A, traces 1 and 2), and the facilitation ratio was ~1.1. However, during N/OFQ exposure, it is evident that the amplitude of the postpulse was greater than that of the prepulse (compare traces 3 and 4), and there is "relief' of N/OFQ-mediated inhibition, as indicated by the elevated facilitation ratio of ~2.0. The time course in Fig. 1A also shows that after recovery of the N/OFQ-mediated Ca^{2+} current inhibition, the neuron was treated for approximately 2 min with UFP-101 (1 μM), and the effect of this peptide blocker on the currents was minimal. Thereafter, the neuron was exposed to both N/OFQ (0.1 μM) and UFP-101 (1 μM) for approximately 60 s, and the N/OFQ-mediated Ca^{2+} current inhibition was blocked (trace 7).

Figure 1B shows a time course of the prepulse and postpulse currents recorded from an SG neuron overexpressing NOP receptors, and the corresponding numbered traces are shown to the right. Unlike the control neuron described, the transfected cell showed an enhanced basal facilitation ratio (~1.5) and tonic voltage-dependent inhibition of Ca^{2+} currents (Fig. 1, A and B; compare traces 1 and 2), indicative of constitutively active NOP receptors. When UFP-101 (1 μM) was applied to the neuron, Ca^{2+} currents were further inhibited in a voltage-dependent manner, similar to that observed

with N/OFQ in control neurons, described above. After a recovery period, the neuron was exposed to N/OFQ (0.1 μM), and the Ca^{2+} current inhibition was greater than that observed with UFP-101. In addition, the recovery period after N/OFQ removal was prolonged compared with the control neuron, presumably a result of the higher expression levels of NOP receptors (discussed below). Figure 1C is a summary graph showing the mean (± S.E.) N/OFQ- and UFP-101-mediated Ca^{2+} current inhibition in control and SG neurons overexpressing NOP receptors. The results show that under control conditions, UFP-101 pretreatment significantly ($P < 0.01$) blocked the N/OFQ-mediated, voltage-dependent Ca^{2+} current inhibition. However, when the NOP receptors were constitutively active, the peptide blocker inhibited Ca^{2+} currents in a voltage-dependent manner. In addition, with the higher NOP receptor expression levels, the N/OFQ-mediated Ca^{2+} current inhibition was greater than that observed for control neurons (compare control and transfected groups, Fig. 1C). These results show that UFP-101 displayed weak partial agonist characteristics under conditions in which heterologously overexpressed NOP receptors are constitutively active.

As noted above, basal facilitation ratio is a measure of tonic G protein activation. Figure 1D shows a scatter plot (horizontal lines denote the mean) of basal facilitation ratios for control and SG neurons transfected with NOP cDNA. The plot shows that when SG neurons were microinjected with cDNA over the range of 10 and 50 ng/μl, the mean facilitation ratio values were not significantly different from control cells. On the other hand, microinjection with concentrations higher than 100 ng/μl resulted in a significantly ($P < 0.001$) higher mean basal facilitation ratio. It should be noted that in this group, most of the neurons were microinjected with 100 to 500 ng/μl cDNA. NOP receptors are coupled to PTX-sensitive G proteins (Mogil and Pasternak, 2001). Thus, in another set of experiments, SG neurons were transfected

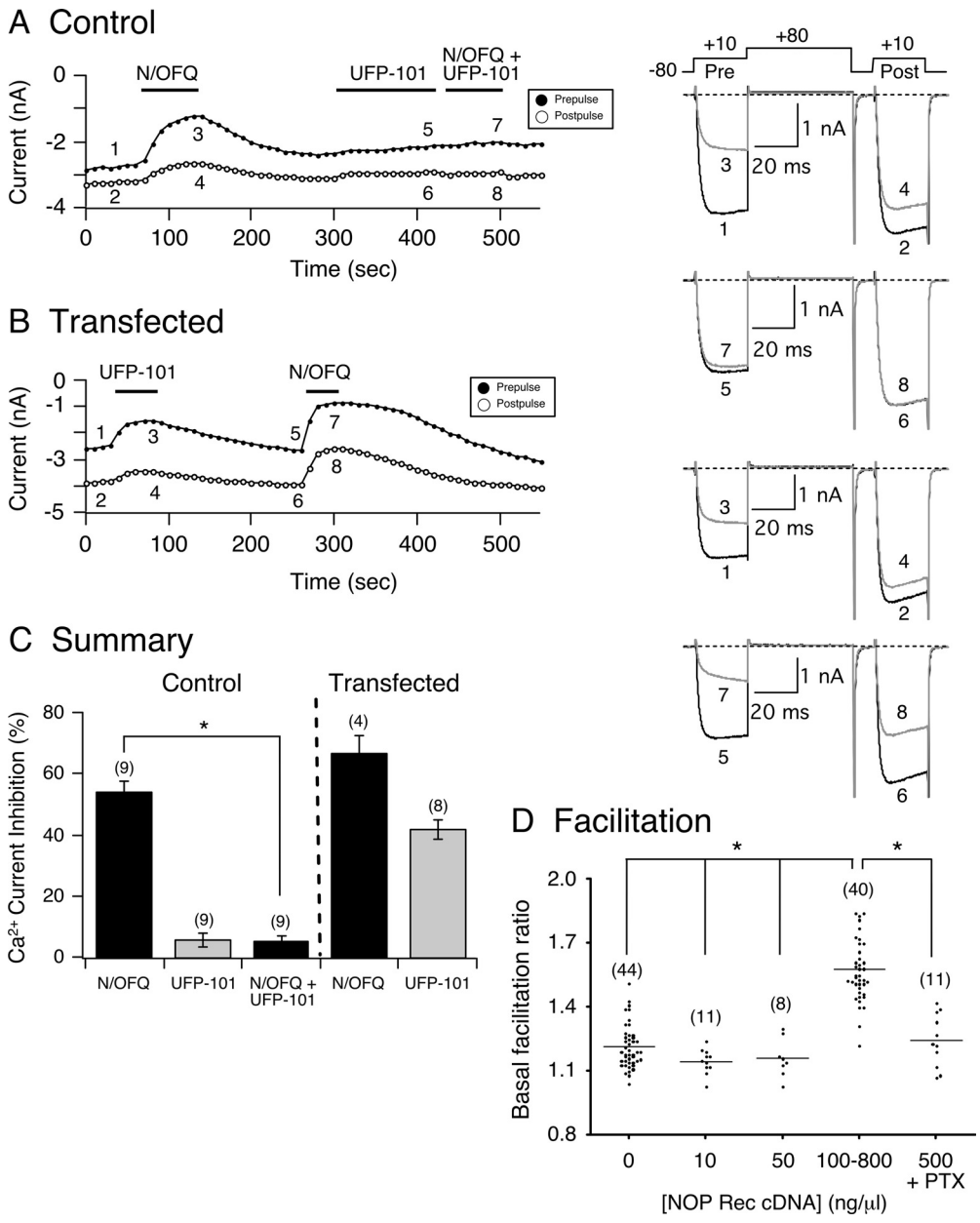

Fig. 1. The peptide UFP-101 exerts weak partial agonist effects on constitutively active NOP receptors. Time courses of Ca^{2+} current amplitude for prepulse (●) and postpulse (○) acquired from the application of N/OFQ (0.1 μM), UFP-101 (1 μM), and N/OFQ + UFP-101 in control (A) and NOP receptor cDNA-transfected SG neurons (B), respectively. Currents were evoked every 10 s with the "double-pulse" voltage protocol (A, top right). The numbered Ca^{2+} current traces in A are shown to the right, where 1 and 2 (black) represent control currents (before N/OFQ exposure), 3 and 4 (gray) represent inhibition at the end of N/OFQ exposure, 5 and 6 (black) represent current amplitude at the end of 2-min UFP-101 (1 μM) exposure, and 7 and 8 (gray) represent inhibition at the end of N/OFQ + UFP-101 exposure. In B, traces 1 and 2 (black) represent control, 3 and 4 (gray) represent inhibition at the end of UFP-101 exposure, 5 and 6 (black) represent current amplitude before N/OFQ application, and 7 and 8 (gray) represent inhibition at the end of N/OFQ exposure. Note that at the beginning of the recordings, the ratio of postpulse to prepulse Ca^{2+} current (e.g., measure of basal facilitation ratio) in B is greater than in the control neuron A, indicating tonic Ca^{2+} current inhibition resulting from NOP receptor overexpression. C, summary graph showing mean ± S.E. Ca^{2+} current inhibition mediated by N/OFQ, UFP-101, and N/OFQ + UFP-101 in control and SG neurons microinjected with NOP receptor cDNA. *, $P < 0.01$ compared with N/OFQ applied alone, paired t test. Numbers in parenthesis indicate the number of neurons tested. D, summary scatter plot of basal facilitation ratio for control neurons and neurons microinjected with NOP cDNA at 10, 50, 100 to 800, and 500 (treated with PTX) ng/μl. Horizontal lines represent the mean, and the numbers in parentheses indicate the number of neurons tested. *, analysis of variance ($P < 0.001$) followed by Newman-Keuls test.

with 500 ng/μl cDNA and pretreated with PTX to determine whether the enhanced G protein-mediated Ca^{2+} channel inhibition would be eliminated. The plot shows that the mean basal facilitation ratio of the PTX-treated neurons was not significantly different from control neurons (Fig. 1D). Therefore, in NOP receptor-transfected neurons, the enhanced basal facilitation ratio correlated with the higher concentrations of microinjected cDNA and was PTX-sensitive.

Trap-101, compound 24, and JTC-801 Display Inverse Agonist Activity in SG Neurons Overexpressing NOP Receptors. Figure 2A shows a time course of current amplitude of a control SG neuron before and during N/OFQ (0.1 μM) application. The superimposed current traces (1–4) are shown on the right. Application of N/OFQ had an effect on Ca^{2+} currents (i.e., voltage-dependent inhibition) similar to that described for control SG neurons in Fig. 1A. After the recovery period, the NOP receptor blocker Trap-101 (1 μM) was applied to the neuron for 3 min, and then both N/OFQ and blocker were reapplied. Traces 5 to 8 (Fig. 2A, right) show that Trap-101 pretreatment abolished the N/OFQ-mediated Ca^{2+} current inhibition. Figure 2B is the time course of the current amplitude of an NOP receptor-transfected neuron exhibiting tonic receptor activation, indicated by the high facilitation ratio (1.55) measured from the amplitude shown for traces 1 and 2. After the application of Trap-101, the amplitude of the prepulse (trace 3) and postpulse (trace 4) currents was increased, and the facilitation ratio decreased to 1.02. After the removal of Trap-101, N/OFQ was applied to the neuron, and the Ca^{2+} currents were inhibited (traces 5–8) in a fashion similar to that observed with transfected neurons with a prolonged recovery period. It is evident that a small tonic inhibition of Ca^{2+} currents remained after N/OFQ removal. In some experiments, it was possible to stably maintain the neurons under our recording conditions and reapply the blockers for an additional 3 min and to determine whether these compounds would revert back to antagonist or inverse agonists after the removal of constitutive receptor activity. Upon re-exposure of Trap-101, the small tonic Ca^{2+} current inhibition was removed (i.e., facilitation ratio changed from 1.12 to 0.95). After the 3-min pretreatment, both N/OFQ and Trap-101 were reapplied, and the N/OFQ-mediated Ca^{2+} current inhibition was blocked

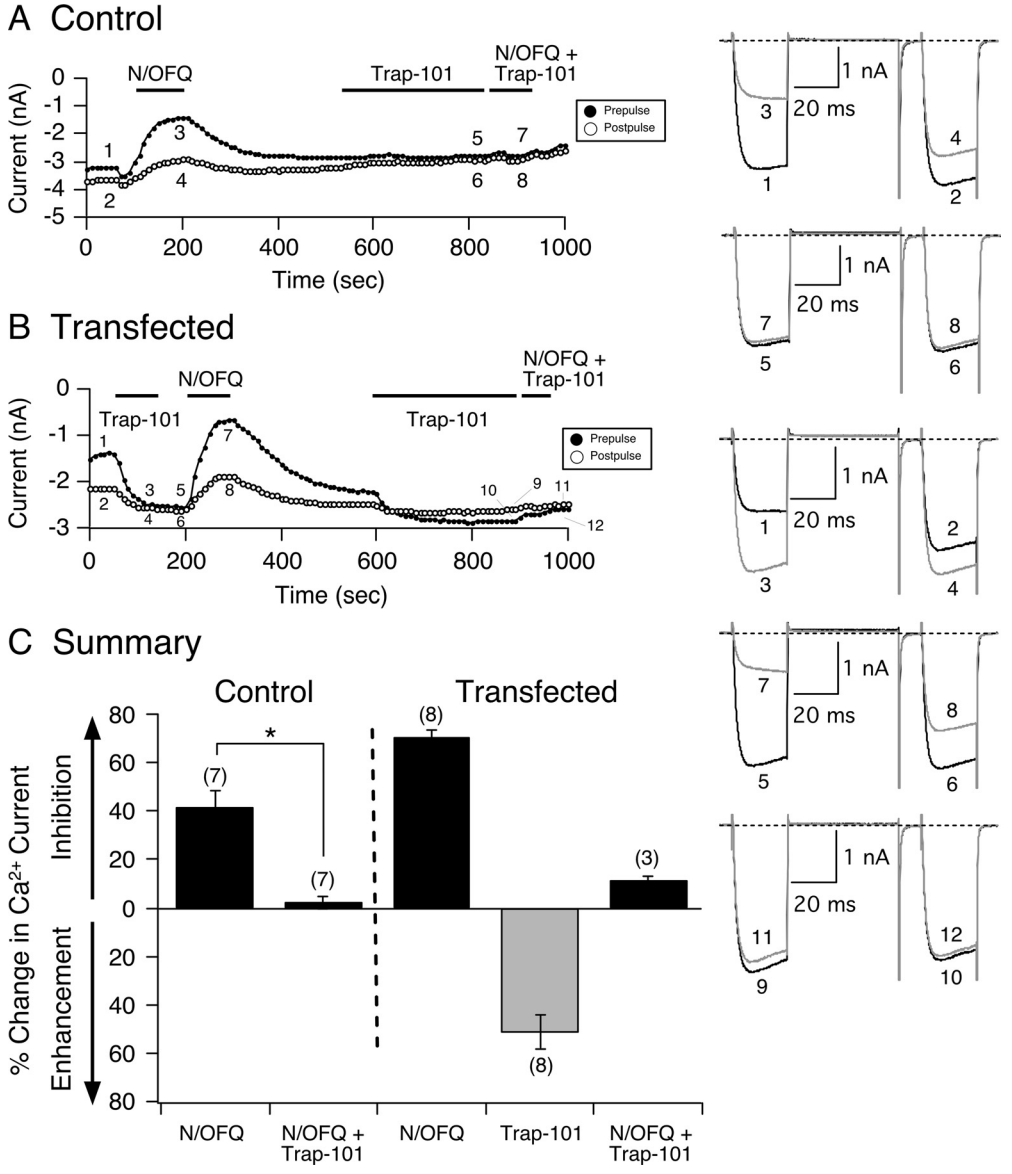

Fig. 2. Trap-101 exerts inverse agonism on constitutively active NOP receptors. Time courses of Ca^{2+} current amplitude for prepulse (●) and postpulse (○) acquired from the application of N/OFQ (0.1 μM), Trap-101 (1 μM), and N/OFQ + Trap-101 in control (A) and NOP receptor cDNA-transfected SG neurons (B), respectively. Currents were evoked every 10 s with the double-pulse voltage protocol (A, top right). The numbered Ca^{2+} current traces in A are shown to the right, where 1 and 2 (black) represent control currents, 3 and 4 (gray) represent inhibition at the end of N/OFQ exposure, 5 and 6 (black) represent current amplitude at the end of a 3-min Trap-101 (1 μM) exposure, and 7 and 8 (gray) represent inhibition at the end of N/OFQ + Trap-101 exposure. In B, traces 1 and 2 (black) represent control currents, 3 and 4 (gray) represent current enhancement at the end of Trap-101 exposure, 5 and 6 (black) represent inhibition before N/OFQ application, 7 and 8 (gray) represent inhibition at the end of N/OFQ exposure, 9 and 10 represent inhibition at the end of a 3-min Trap-101 application, and 11 and 12 (gray) represent inhibition at the end of N/OFQ + Trap-101 exposure. C, summary graph showing mean ± S.E. percentage of change in Ca^{2+} current inhibition or enhancement mediated by N/OFQ, Trap-101, and N/OFQ + Trap-101 in control and transfected SG neurons. *, $P < 0.01$ compared with N/OFQ applied alone, paired t test. Numbers in parentheses indicate the number of neurons tested.

(traces 9–12), similar to that observed with control neurons (Fig. 1A). Figure 2C is a summary plot of the percentage of change in Ca^{2+} current measured in both control and NOP receptor-transfected SG neurons. In control neurons, Trap-101 significantly ($P < 0.01$) blocked the N/OFQ-mediated Ca^{2+} current inhibition without showing any intrinsic activity (Fig. 2C). However, the summary plot also shows that when NOP receptors were constitutively active in transfected neurons, Trap-101 enhanced the Ca^{2+} current amplitude by more than 50% but retained its blocking ability once the receptors were silent ($n = 3$ recordings).

In the next set of experiments, the lipid-soluble NOP receptor blocker compound 24 was tested for its ability to affect constitutively active NOP receptors. Compound 24 has been reported to exhibit the highest ranking order of antagonist potency for NOP receptors (Fischetti et al., 2009). Figure 3A shows the time course for a control neuron before (traces 1 and 2) and during (traces 3 and 4) exposure to N/OFQ (0.1 μM), compound 24 (1 μM, traces 5 and 6), and both compounds together (traces 7 and 8). Similar to the results described above, when N/OFQ was applied to the external solution, Ca^{2+} currents were inhibited in a voltage-dependent manner. Pretreatment of the neuron with compound 24 for 3 min did not have an overt effect on the Ca^{2+} current amplitude. However, when both agonist and blocker were coapplied, the N/OFQ-mediated Ca^{2+} current inhibition was blocked. The time course shown in Fig. 3B is that of an SG neuron heterologously expressing NOP receptors with an enhanced basal facilitation ratio (Fig. 3B, traces 1 and 2, right). After a 50-s application of compound 24, the Ca^{2+} current amplitude for both prepulse and postpulse was enhanced (traces 3 and 4), and the basal facilitation ratio decreased to 1.08. Thereafter, N/OFQ (0.1 μM) was applied, and the Ca^{2+} current inhibition was greater compared with the control neuron (Fig. 3A) and, as expected, exhibited a longer recovery period. When compound 24 was reapplied again for 3 min and then coapplied with N/OFQ, the agonist-mediated Ca^{2+} current inhibition was abolished. This effect of com-

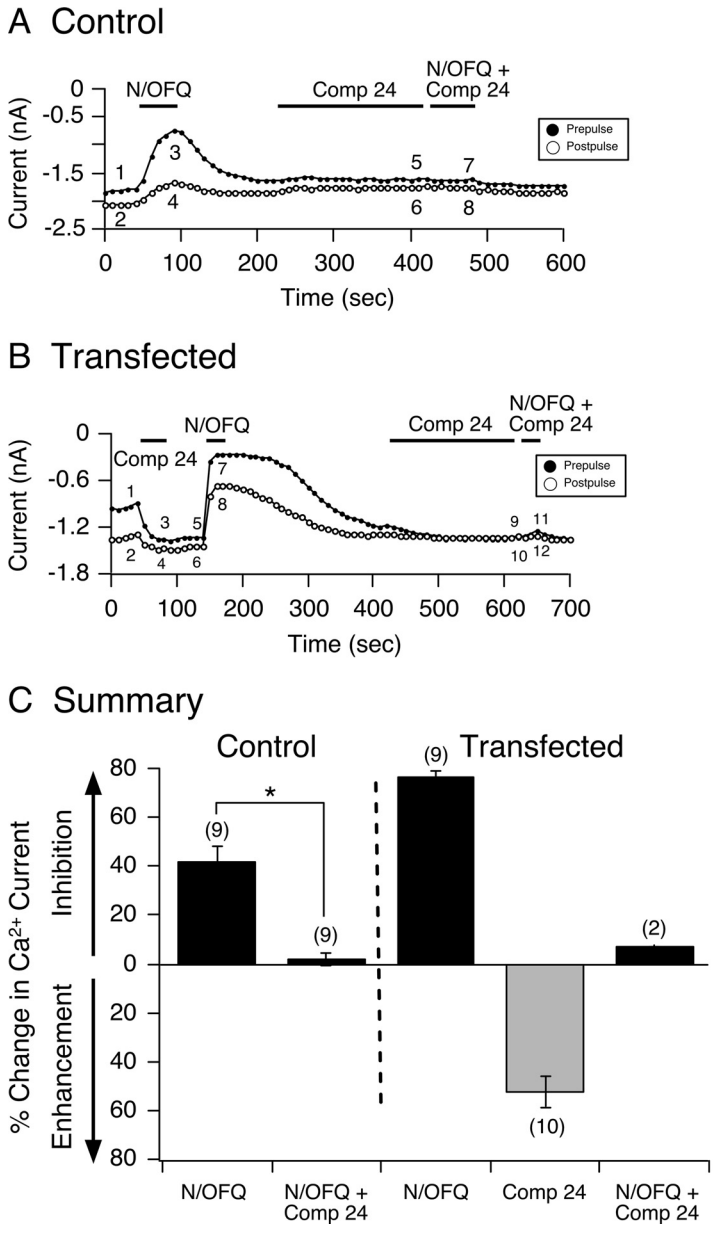

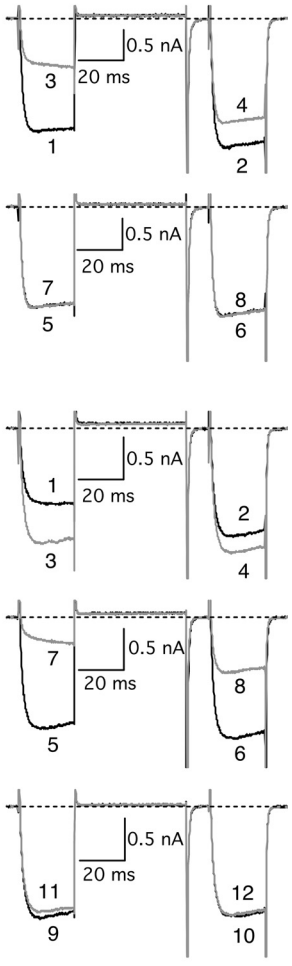

Fig. 3. Compound 24 exerts inverse agonism on constitutively active NOP receptors. Time courses of Ca^{2+} current amplitude for prepulse (●) and postpulse (○) acquired from the application of N/OFQ (0.1 μM), compound 24 (1 μM), and N/OFQ + compound 24 in control (A) and NOP receptor cDNA-transfected SG neurons (B), respectively. Currents were evoked every 10 s with the double-pulse voltage protocol (A, top right). The numbered Ca^{2+} current traces in A are shown to the right, where 1 and 2 (black) represent control currents, 3 and 4 (gray) represent inhibition at the end of N/OFQ exposure, 5 and 6 (black) represent current amplitude at the end of a 3-min compound 24 (1 μM) exposure, and 7 and 8 (gray) represent inhibition at the end of N/OFQ + compound 24 exposure. In B, traces 1 and 2 (black) represent control currents, 3 and 4 (gray) represent current enhancement at the end of compound 24 exposure, 5 and 6 (black) represent amplitude before N/OFQ application, 7 and 8 (gray) represent inhibition at the end of N/OFQ exposure, 9 and 10 (black) represent amplitude at the end of a 3-min compound 24 exposure, and 11 and 12 (gray) represent inhibition at the end of N/OFQ + compound 24 exposure. C, summary graph showing mean ± S.E. (except for N/OFQ + compound 24, $n = 2$) percentage change in Ca^{2+} current inhibition or enhancement mediated by N/OFQ and compound 24 in control and transfected SG neurons. *, $P < 0.01$ compared with N/OFQ applied alone, paired t test. Numbers in parentheses indicate the number of neurons tested.

pound 24 was observed in two transfected neurons in which we were able to obtain longer stable recordings. The summary plot in Fig. 3C shows that in transfected cells, compound 24 enhanced the Ca^{2+} current amplitude by approximately 52% when NOP receptors were constitutively active but significantly ($P < 0.01$) inhibited the N/OFQ-mediated Ca^{2+} current inhibition in control neurons.

The lack of N/OFQ-mediated Ca^{2+} current inhibition during the second application in the presence of the blockers in transfected neurons shown in both time courses (Fig. 2, B and B) prompted us to perform a separate set of experiments as negative controls to rule out NOP receptor desensitization. Seven SG neurons were transfected with NOP receptor cDNA (500 ng/μl) and exposed initially to compound 24 (1 μM). After the recovery period, N/OFQ (0.1 μM) was applied to bath solution until maximal Ca^{2+} current inhibition occurred. Once recovery from N/OFQ was reached, the control external solution was used to perfuse the cells for an additional 3 min. Thereafter, the SG neurons were re-exposed to N/OFQ. Under these conditions, the mean (± S.E.) Ca^{2+} current inhibition (percentage) was 62.5 ± 4.9 and 65.7 ± 3 during the first and second N/OFQ application, respectively ($P = 0.26$, not significant; data not shown). These results suggest that in transfected neurons, the lack of coupling between Ca^{2+} channels and NOP receptors after the 3-min antagonist exposure was probably a result of receptor block rather than receptor desensitization.

Figure 4, A and B, show the time courses for a control and an NOP receptor-expressing neuron, respectively. As described for the blockers above, in control SG neurons, JTC-801 (1 μM) was applied to the external bath solution for 3 min. JTC-801 is a lipophilic and high-affinity NOP receptor antagonist (Shinkai et al., 2000). Traces 7 and 8 (Fig. 4A, right) show that the receptor blocker abolished the N/OFQ-mediated inhibition of Ca^{2+} currents. Figure 4B is the time course of current amplitude for prepulse and postpulse currents from a transfected SG neuron with a basal facilitation of 1.69. Similar to Trap-101 and compound 24, exposure of the neuron to the blocker resulted in an enhancement of both prepulse and postpulse current amplitude (traces 1–4). In

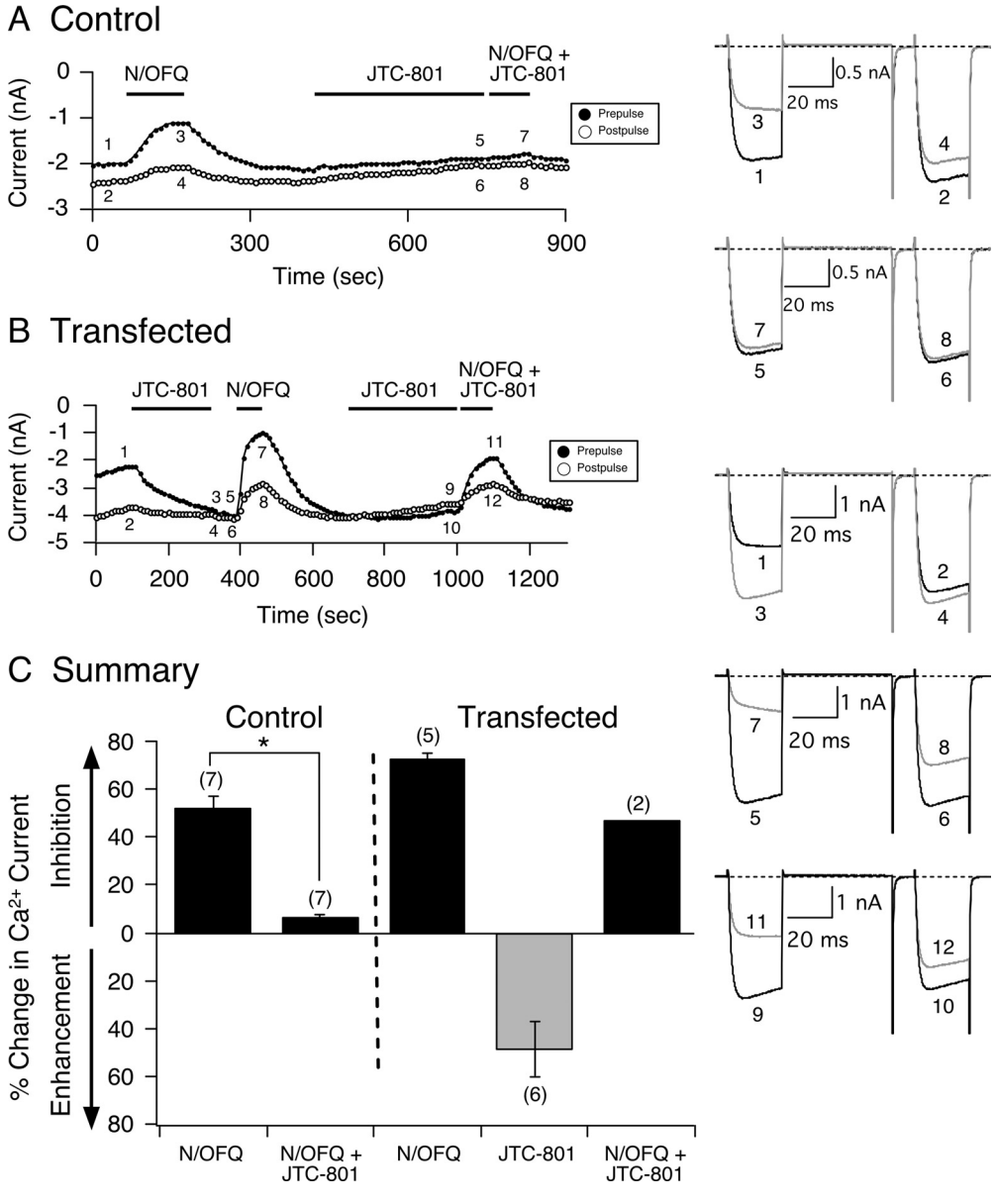

Fig. 4. JTC-801 exerts inverse agonism on constitutively active NOP receptors. Time courses of Ca^{2+} current amplitude for prepulse (●) and postpulse (○) acquired from the application of N/OFQ (0.1 μM), JTC-801 (1 μM), and N/OFQ + JTC-801 in control (A) and NOP receptor cDNA-injected SG neurons (B), respectively. Currents were evoked every 10 s with the double-pulse voltage protocol (A, top right). The numbered Ca^{2+} current traces in A are shown to the right, where 1 and 2 (black) represent control, 3 and 4 (gray) represent inhibition at the end of N/OFQ exposure, 5 and 6 (black) represent current amplitude at the end of 3-min JTC-101 (1 μM) exposure, and 7 and 8 (gray) represent inhibition at the end of N/OFQ + JTC-801 exposure. In B, traces 1 and 2 (black) represent control currents, 3 and 4 (gray) represent enhancement at the end of JTC-801 exposure, 5 and 6 (black) represent amplitude before N/OFQ application, 7 and 8 (gray) represent inhibition at the end of N/OFQ exposure, 9 and 10 (black) represent amplitude at the end of a 3-min JTC-801 exposure, and 11 and 12 (gray) represent inhibition at the end of N/OFQ + JTC-801 exposure. C, summary graph showing mean ± S.E. (except for N/OFQ + JTC-801, $n = 2$) percentage change in Ca^{2+} current inhibition or enhancement mediated by N/OFQ and JTC-801 in control and transfected SG neurons. *, $P < 0.01$ compared with N/OFQ applied alone, paired t test. Numbers in parentheses indicate the number of neurons tested.

addition, once JTC-801 was removed, the tonic Ca^{2+} current inhibition was eliminated, and the basal facilitation ratio decreased to 1.03. After a 3-min pretreatment with JTC-801, coapplication of the blocker and N/OFQ resulted in a voltage-dependent inhibition of the Ca^{2+} currents that was lower in magnitude than that observed with the initial N/OFQ application (compare traces 7, 8, 11, and 12). The inability of JTC-801 to completely block the agonist-mediated current inhibition during the second application in transfected neurons was observed in two neurons under conditions in which long recordings were possible. As shown in the summary plot in Fig. 4C, JTC-801 significantly ($P < 0.01$) blocked the N/OFQ-mediated Ca^{2+} current inhibition in control neurons, but it exerted inverse agonist effects on constitutively active NOP receptors in transfected SG neurons. Overall, these results show that these four NOP receptor ligands that behave as pure antagonists in control SG neurons display distinct pharmacological activities in neurons overexpressing NOP receptors: either partial agonism (i.e., UFP-101) or inverse agonism (Trap-101, compound 24, and JTC-801).

Na^+ Ions Modulate the Pharmacological Profile of N/OFQ-Activated Native NOP Receptors and Ca^{2+} Channels. In the next series of experiments, we examined the effect of varying Na^+ ion concentrations on the N/OFQ concentration-response relationship in SG neurons. The time course of Ca^{2+} current amplitude for prepulse and postpulse current acquired with the double-pulse voltage protocol (Fig. 5B, top) shows the effect of switching external solution from 0 to 120 mM Na^+ with the NMG internal solution (Fig. 5A). NMG was the major monovalent cation in the external solution in which Na^+ was absent and was substituted for an equimolar amount of Na^+ in the 120 mM Na^+ external solution. $NaMeSO_3$ rather than NaCl was used in the external solutions to maintain equal Cl^- ion concentrations in both internal and external solutions (20 mM) with a predicted reversal potential of Cl^- currents at 0 mV (Zhu and Ikeda, 1993) and to avoid contamination of Ca^{2+}-activated Cl^- currents expressed in sympathetic neurons (De Castro et al., 1997). Nevertheless, in some experiments, NaCl was used, and similar results were observed (data not shown). Figure 5B shows the superimposed Ca^{2+} current traces obtained before and during exposure to 120 mM Na^+. After exposure to 120 mM Na^+, the peak Ca^{2+} current amplitude decreased approximately 10%. Figure 5C shows the current-voltage (I-V) relationships for the step current from the neuron in Fig. 5A before (●) and during (○) Na^+ application. In the presence of Na^+, the amplitude of the step currents decreased at step potentials between −15 and +50 mV. As shown in Fig. 5C, the change in peak amplitude (+10 mV) was not a result of a shift in the I-V relationship.

In addition, traces 3 and 4 in Fig. 5B show that applying 120 mM Na^+ resulted in the appearance of a tail current after repolarization to −80 mV (dashed circle). This contaminating current is reminiscent of that studied previously in

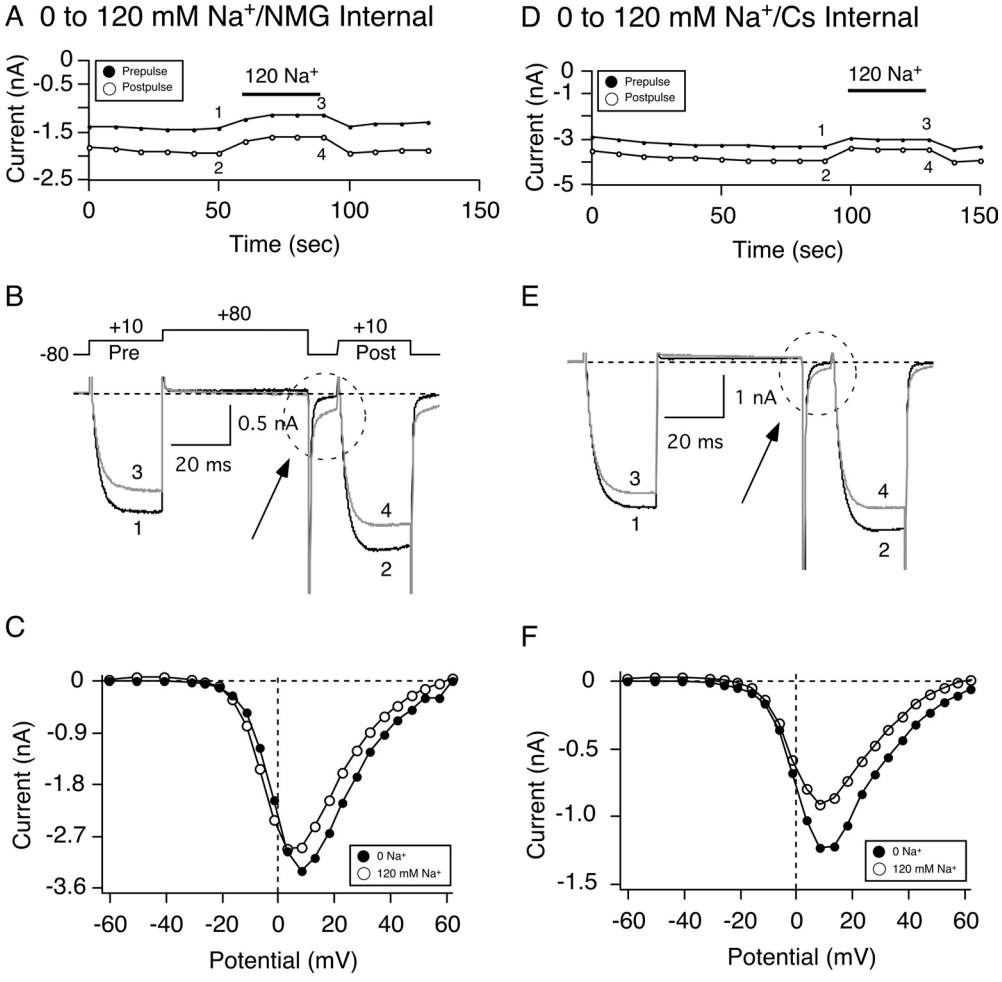

Fig. 5. Switching external solutions from 0 to 120 mM Na^+ leads to a reduction in peak Ca^{2+} current. Time courses of Ca^{2+} current amplitude inhibition for prepulse (●) and postpulse (○) acquired while switching external solutions from 0 to 120 mM Na^+ with either "NMG" (A) or "Cs^+" internal (D) solutions. Ca^{2+} currents were evoked every 10 s with the double-pulse voltage protocol (B, top). The numbered Ca^{2+} current traces in A and D are shown at the bottom of each time course. Current traces represent current amplitude before (1 and 2, black) and during (3 and 4, gray) Na^+ exposure. The broken circles in B and E point to a tail current carried by Na^+. I-V curves for the neurons in A and B are shown in E and F before (●) and during (○) 120 mM Na^+ exposure. Currents were elicited by a 70-ms depolarizing pulse from a holding potential of −80 mV to potential ranging from −60 to 60 mV.

rat sympathetic neurons and shown to result from Na^+ ions going through K^+ channels that was blocked by external Ba^{2+} or quinidine or internal Cs^+ (Zhu and Ikeda, 1993). Thus, we used an internal solution containing 40 mM Cs^+ to block this contaminating Na^+ current. Figure 5D is a time course of Ca^{2+} current amplitude of an SG neuron in which the external solution was switched from 0 to 120 mM Na^+ with a Cs^+-containing internal solution. Similar to the cell in Fig. 5A, applying 120 mM Na^+ led to a decrease in peak Ca^{2+} current amplitude (traces 1–4, Fig. 5E) without a shift in the I-V relationship (Fig. 5F). In nine SG neurons, the mean (± S.E.) decrease in Ca^{2+} current amplitude (at +10 mV) decreased 18.1 ± 1.0% (Fig. 7B). In addition, the presence of Cs^+ in the internal solution blocked a considerable amount of the putative contaminating Na^+ current (compare Fig. 5, B and E, dashed circles).

The N/OFQ concentration-response relationship was measured next under conditions in which the external Na^+ concentration was varied. Figure 6, A and B, show the time courses of peak Ca^{2+} current in SG neurons after the sequential exposure of 0.03 and 3 μM N/OFQ in the absence or presence of 120 mM Na^+, respectively. The numbered traces for each time course are shown to the right. It can be seen that application of 0.03 μM N/OFQ led to a greater Ca^{2+} current inhibition in the presence of 120 mM Na^+ compared with the absence of Na^+. The effect of 3 μM N/OFQ also led to a slightly higher N/OFQ-mediated Ca^{2+} current inhibition when Na^+ was present in the external solution (compare Fig. 6, A and B, traces 5–8). The results of the N/OFQ concentration-response curves in different Na^+ concentrations are plotted in Fig. 6C. The data points were fitted to the Hill equation, and the IC_{50} (nanomolar), Hill coefficient (± S.E.), and maximum current inhibition (percentage ± S.E.) values obtained, respectively, were 95, 157, 76, and 74; 2.15 ± 0.42,

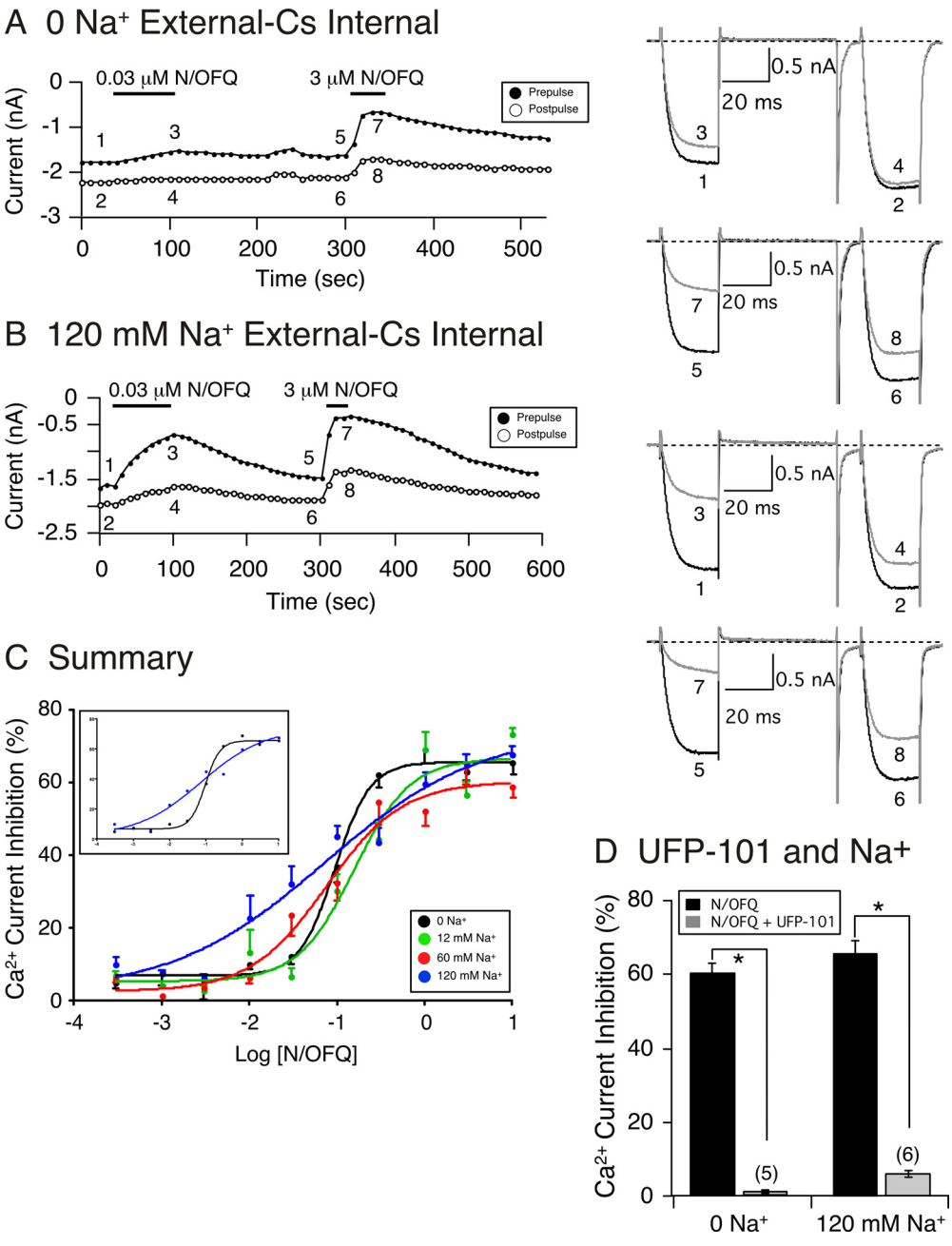

Fig. 6. External Na^+ causes leftward shifts of the N/OFQ concentration-response relationships. Time courses of Ca^{2+} current amplitude inhibition for prepulse (●) and postpulse (○) acquired from the sequential application of 0.03 and 3 μM N/OFQ in SG neurons in 0 (A) and 120 mM Na^+ (B). Currents were evoked every 10 s with the double-pulse voltage protocol (top Fig. 5B). The numbered Ca^{2+} current traces in A and B are shown to the right. Black traces represent control current amplitudes and gray traces represent current amplitude in the presence of N/OFQ. C, concentration-response curves in SG neurons exposed to N/OFQ in 0 (black circles), 12 (green circles), 60 (red circles), and 120 (blue circles) mM Na^+-containing external solutions. Each data point represents the mean (± S.E., n = 4–19) prepulse Ca^{2+} current inhibition. The smooth curves were obtained by fitting the points to the Hill equation. The inset shown is a replicate of the data and curve fits for SG neurons exposed to N/OFQ in 0 and 120 mM Na^+ to highlight the effect of the cation. D, summary graph showing mean ± S.E. Ca^{2+} current inhibition mediated by N/OFQ in SG neurons in 0 and 120 mM Na^+ during application of N/OFQ (■) and N/OFQ + UFP-101 (■). *, $P < 0.01$ compared with N/OFQ applied alone, paired t test. Numbers in parentheses indicate the number of neurons tested.

1.35 ± 0.57, 1.0 ± 0.27, and 0.49 ± 0.20; and 74.1 ± 10.0, 60.2 ± 3.1, 66.5 ± 3.1, 65.6 ± 1.4% for 0, 12, 60, and 120 mM Na^+, respectively. The plots in Fig. 6C show that increasing external Na^+ (except for 12 mM Na^+) led to a slight leftward shift in Ca^{2+} current inhibition (i.e., increased in potency) that was accompanied by a robust decrease in Hill coefficient values. Statistical comparison between the fits showed that compared with 0 Na^+, the Hill coefficients for 60 and 120 mM Na^+ were significantly different, with P values of 0.039 and 0.001, respectively. However, the efficacy of N/OFQ was not significantly different between any of the groups tested. The inset in Fig. 6C is a plot of the data for 0 and 120 mM Na^+ to highlight both the leftward shift in IC_{50} for 120 mM Na^+ and the shallow fit of the curve. These results show that increasing external Na^+ ion concentration slightly increased the N/OFQ potency for NOP receptors, decreased the Hill coefficient more than 4-fold, and exerted minimal effects on the agonist efficacy.

Although the presence of external Na^+ has also been shown to increase the affinity of blockers for GPCR, including NOP receptors, we hypothesized that the ability of UFP-101 to block the N/OFQ-mediated Ca^{2+} current inhibition would be diminished in the presence of Na^+, given the increased potency of N/OFQ described for Fig. 6C. Thus, in the next set of experiments, we examined whether the blocking effect of UFP-101 (as shown in Fig. 1C) would be altered in the presence of 120 mM Na^+. Figure 6D is a summary plot comparing the N/OFQ-mediated Ca^{2+} current inhibition in the absence and presence of 120 mM Na^+. The results show that the ability of UFP-101 to block NOP receptor activation was not affected with the addition of Na^+ (compare Figs. 1C and 6D).

Allosteric Modulation of Na^+ Ions on the Coupling of Constitutively Active NOP Receptors with Ca^{2+} Channels. Next, we examined the effect of Na^+ ion exposure of SG neurons exhibiting constitutively active NOP receptors. Figure 7A is a time course of the Ca^{2+} current amplitude recorded from an SG neuron transfected with NOP receptor cDNA. As described above for NOP receptor-transfected neurons, the cell exhibited an elevated basal facilitation ratio (traces 1 and 2). After exposure to 120 mM Na^+, the prepulse Ca^{2+} current amplitude rapidly (~20 s) increased, the tonic Ca^{2+} channel inhibition was removed (traces 3 and 4), and the facilitation ratio decreased to 1.07. After the removal of Na^+, the tonic current inhibition returned quickly (~20 s), and the prepulse current amplitude decreased, which resulted in a return of the higher facilitation ratio. The time course also shows that application of 60 or 12 mM Na^+ led to enhancement of the prepulse Ca^{2+} current amplitude, as observed with 120 mM Na^+. After a recovery period for 12 mM Na^+, 0.1 μM N/OFQ was applied, and the Ca^{2+} currents were inhibited in a voltage-dependent manner (Fig. 7A, traces 7 and 8). Note that the recovery period was prolonged, as described for NOP-receptor transfected neurons shown in Figs. 1 to 4. The summary graph in Fig. 7B shows that unlike control SG neurons, in which application of external Na^+ led to an 18% inhibition of peak Ca^{2+} currents, exposure of transfected cells to 120 mM Na^+ resulted in an enhancement of the Ca^{2+} currents accompanied by the loss of the elevated basal facilitation ratio. As described for the four blockers above, application of N/OFQ resulted in a greater inhibition of Ca^{2+} currents in transfected neurons compared with the control group. These results suggest that in control neurons, the Na^+-mediated decrease in peak Ca^{2+} current amplitude was presumably a result of cation selectivity (i.e., Ca^{2+} versus Na^+). On the other hand, in transfected neurons, the Na^+-mediated loss of enhanced basal facilitation ratio resulted from the removal of the steady-state G$\beta\gamma$-mediated Ca^{2+} channel inhibition.

One marked difference between the effect of Na^+ ions and the three blockers exerting inverse agonism was that the removal of the elevated basal facilitation by the former was reversible whereas that of the latter was not. In addition, as mentioned above, the magnitude of the N/OFQ-mediated Ca^{2+} current inhibition in NOP receptor-transfected neurons was greater than control cells. One possibility could be that in transfected neurons, the "excess" level of expressed NOP receptors could result in the coupling to other Ca^{2+} channel subtypes rather than restricted to N-type Ca^{2+} channels. We have shown previously that in SG neurons, approximately 65% of Ca^{2+} current is carried by N-type channels, with 15 and 10%, respectively, by P/Q- and L-type channels (Fuller et al., 2004). Thus, in the next set of experiments, we examined the effect of blocking N-type Ca^{2+} channels with the specific toxin, ω-conotoxin GVIA (10 μM), on enhanced Ca^{2+} current inhibition (i.e., basal facilitation ratio). Figure 7C shows a time course of a peak Ca^{2+} current in a control cell with a basal facilitation ratio of 1.14 (see traces 1 and 2, right). Prepulse and postpulse Ca^{2+} currents were evoked as described above. Exposure of the cell to the toxin for 3 min resulted in an inhibition of the prepulse current from 3.7 to 1.3 nA (65% block, traces 1–4). In addition, the facilitation ratio decreased to 0.93. Immediately after removing the toxin, N/OFQ (0.1 μM) was applied to the neuron for 50 s, and coupling between NOP receptors and Ca^{2+} channels was completely abolished (traces 5 and 6). Figure 7D also shows that application of the toxin to a transfected neuron (basal facilitation ratio, ~1.5) also led to a block of the prepulse current from 2.1 to 0.8 nA (63% current block) and a decrease of the enhanced facilitation ratio to 0.98. However, when N/OFQ was applied immediately to the cell after toxin removal, the Ca^{2+} current was further inhibited. In five control cells, the N/OFQ-mediated Ca^{2+} current inhibition after the 3-min toxin incubation was 1 ± 2% (± S.E.), whereas in NOP receptor-transfected neurons, the current inhibition was 19 ± 2% (±S.E., n = 8). These results suggest that in transfected neurons, the enhanced basal facilitation ratio is mediated by tonic N-type Ca^{2+} channel inhibition, and the elevated N/OFQ-mediated current inhibition results from coupling of "excess" NOP receptors with ω-conotoxin-insensitive Ca^{2+} channels.

Na^+ also Exerts Allosteric Modulation in Constitutively Active MOP Receptors. In the final set of experiments, MOP receptors were heterologously expressed in SG neurons to determine whether the overexpressed receptors would also exhibit constitutive activity and tonically inhibit Ca^{2+} channel currents as demonstrated with NOP receptors. We have reported previously that this opioid receptor subtype is not normally expressed in this neuron type (Ruiz-Velasco et al., 2005). Figure 8A shows the time course of the Ca^{2+} current amplitude of an SG neuron overexpressing MOP receptors. Similar to the NOP receptor overexpression results, this opioid receptor subtype displayed constitutive activity as illustrated by the elevated basal facilitation ratio of 2.0 (traces 1 and 2).

Exposure to 120 mM Na^+ led to rapid (within 20 s) enhancement of the Ca^{2+} currents from 1.1 to 3.1 nA (traces 3 and 4). After the removal of Na^+, the basal facilitation ratio returned to the enhanced level. Thereafter, the MOP blocker CTAP (10 μM) was applied to the neuron, and the facilitation ratio decreased to 1.12. In essence, CTAP exerted inverse agonism similar to that described for NOP receptor antagonists above. Furthermore, when DAMGO (1 μM) and CTAP (10 μM) were applied to the cell, the coupling between MOP receptors and Ca^{2+} currents was abolished (traces 7 and 8). The summary graph in Fig. 8B shows that in MOP receptor-expressing SG neurons, application of DAMGO alone resulted in a 45% inhibition of Ca^{2+} currents. On the other hand, exposure to either CTAP or Na^+ ions alone led to an enhancement of Ca^{2+} currents and removal of the elevated basal facilitation ratio. These results suggest that the allosteric modulation of Ca^{2+} currents and inverse agonism observed with Na^+ and receptor blockers, respectively, are common to both constitutively active NOP and MOP receptors in SG neurons.

Discussion

The purpose of the present study was to heterologously express NOP receptors in acutely isolated SG neurons to confer upon the receptors a constitutively active state and compare the pharmacological profile of four high-affinity receptor blockers and the allosteric effects of Na^+ ions on the

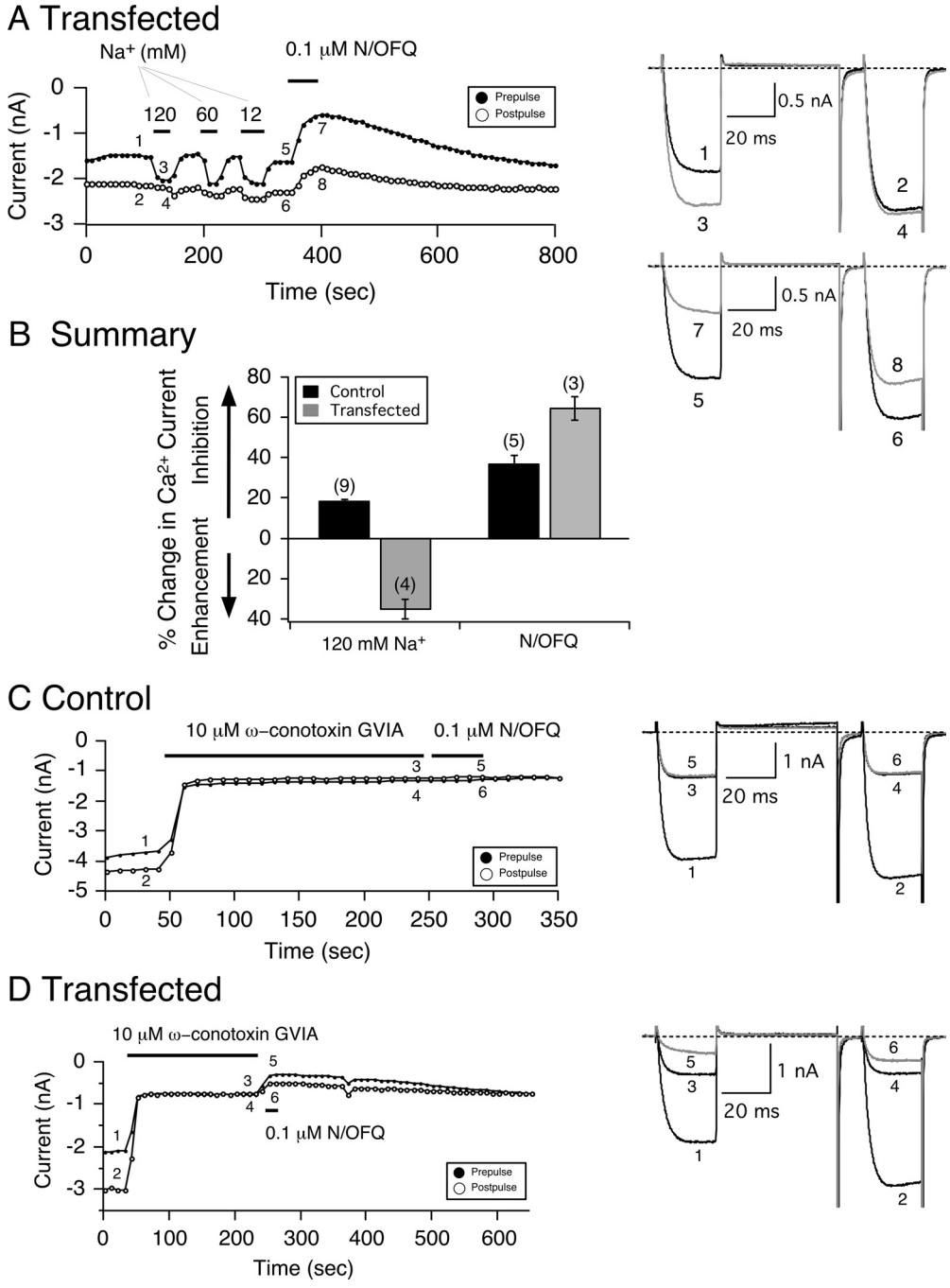

Fig. 7. Constitutively active (A) NOP receptors heterologously overexpressed in SG neurons are modulated by Na^+ ions. Time course of Ca^{2+} current amplitude inhibition for prepulse (●) and postpulse (○) acquired from the sequential application of 120, 60, and 12 mM Na^+ and 0.1 μM N/OFQ in SG neurons microinjected with NOP receptor cDNA (A). Currents were evoked every 10 s with the double-pulse voltage protocol (top Fig. 5B) in the absence (black traces) or presence (gray traces) of either Na^+ or N/OFQ. The numbered Ca^{2+} current traces in A are shown to the right. B, summary graph of mean (± S.E.) percentage change in Ca^{2+} current produced by Na^+ (120 mM) and N/OFQ (0.1 μM). The percentage change was determined from the Ca^{2+} current amplitude measured isochronally at 10 ms into the prepulse (+10 mV) in the absence and presence of agonist in control (■) and NOP receptor-transfected (■) SG neurons. Numbers in parenthesis indicate the number of experiments. Time courses of peak Ca^{2+} current amplitude for prepulse and postpulse acquired from the sequential application of ω-conotoxin GVIA (10 μM, gray traces) and N/OFQ (0.1 μM) in control (C) and NOP receptor-transfected (D) SG neurons. Currents were evoked every 10 s as in A. The numbered Ca^{2+} current traces in C and D are shown to the right.

N/OFQ-mediated Ca^{2+} current inhibition. Previous studies have shown that NOP receptors are natively expressed in SG neurons (Ruiz-Velasco et al., 2005; Margas et al., 2008). Thus, this model system was ideal to compare the effects of antagonists or Na^+ ions under conditions in which NOP receptors are silent (i.e., physiological expression levels) or constitutively active (i.e., high expression levels) within a neuronal environment. In control SG neurons, all four blockers significantly eliminated the N/OFQ-mediated Ca^{2+} current inhibition, and more importantly, did not exhibit an intrinsic activity when NOP receptors were silent. On the other hand, in SG neurons overexpressing NOP receptors, UFP-101 displayed weak partial agonist effects, whereas Trap-101, compound 24, and JTC-801 exerted inverse agonist effects. That NOP receptor levels affect agonist responses has been reported by Lambert and coworkers (McDonald et al., 2003; Barnes et al., 2007). They used an ecdysone-inducible expression Chinese hamster ovary cell system to control receptor expression levels. They reported that the peptide partial agonist [F/G]N/OFQ(1-13)-NH_2 exhibited partial and full agonism as well as antagonism under different receptor density levels. Our findings now extend these observations to show that NOP receptor antagonists can also exert differential effects that are dependent on expression levels and receptor activity. That is, when constitutively active NOP receptors were exposed to lipid-soluble blockers (Trap-101, compound 24, and JTC-801), inverse agonism was observed, and tonic receptor activation was removed. Upon a subsequent re-exposure of the same compound for 3 min, the N/OFQ-mediated Ca^{2+} current inhibition was blocked similarly to that observed in control neurons, although JTC-801 did not fully block the response in two cells tested. It may be that a longer incubation period may have been required with this antagonist. Indeed, it has been reported that this compound exerted a time-dependence with regard to blocking the N/OFQ-mediated [^{3}H]norepinephrine overflow in rat neocortex-derived synaptosomes (Marti et al., 2003).

To our knowledge, this is the first study to demonstrate that the pharmacological profile of NOP receptor blockers is altered when the receptors are constitutively active. For instance, UFP-101 has been shown to exhibit potent NOP receptor blocking effects both in vitro and in vivo (Calo et al., 2005). Our results suggest that the high receptor expression levels amplify some residual agonist activity of this ligand that is normally undetectable at physiological levels. It is noteworthy in this context that the potency of the NOP receptor blocker [Nphe^1]N/OFQ(1-13)NH_2 (Nphe^1 is the chemical modification that confers antagonist properties upon UFP-101) has been reported to be modulated by Na^+ and GTP such that it can exhibit agonist-like properties (Olianas and Onali, 2003). It should also be pointed out that the three lipid-soluble compounds used in this study have a diverse chemical structure. Trap-101 is an achiral analog of the NOP receptor blocker J-113397 that belongs to a class of benzimidazolinones (Trapella et al., 2006). Compound 24 is a spiropiperidine compound that, thus far, ranks highest among the NOP receptor blockers (Goto et al., 2006; Fischetti et al., 2009), and JTC-801 is a small-molecule 4-aminoquinoline (Shinkai et al., 2000). Inverse agonism exerted by these compounds suggests that there is a common structural feature to Trap-101, compound 24, and JTC-801 that influences their interaction with NOP receptors. Further studies are necessary to define these crucial structural features. Never-

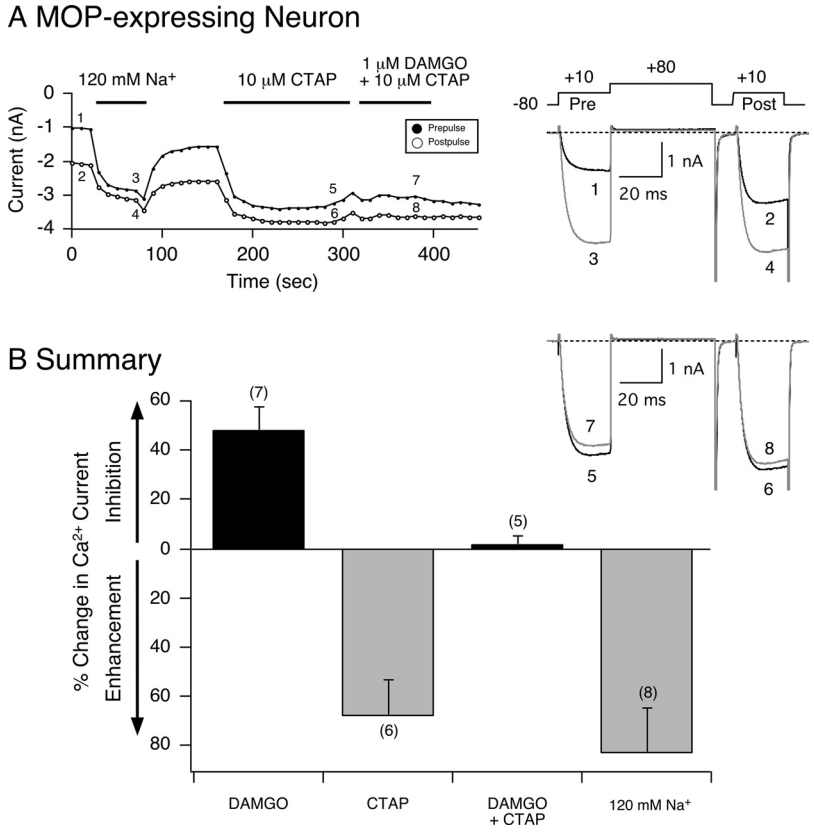

Fig. 8. Na^+ ion-mediated allosteric effects and CTAP inverse agonism on constitutively active MOP receptors heterologously expressed in SG neurons. A, time course of peak Ca^{2+} current amplitude inhibition for prepulse (●) and postpulse (○) currents before and during exposure to DAMGO (1 μM), CTAP (10 μM), DAMGO + CTAP, and 120 mM Na^+. Ca^{2+} currents were evoked every 10 s with the double-pulse voltage protocol (A, top right) in the absence (black traces 1 and 2, 5 and 6) or presence (gray traces 3 and 4, 7, and 8) of 120 mM Na^+ and DAMGO + CTAP, respectively. B, summary graph of mean (± S.E.) percentage change in Ca^{2+} current produced by DAMGO, CTAP, DAMGO + CTAP, and external Na^+ (120 mM) in MOP receptor-expressing SG neurons. The percentage change was determined from the Ca^{2+} current amplitude measured isochronally at 10 ms into the prepulse (+10 mV) in the absence and presence of compound. Numbers in parentheses indicate the number of experiments.

theless, it is possible that the findings described above may serve as the basis for the design of a pharmacophore as discussed previously (Zaveri et al., 2005).

One of the limitations of the approach used in this study is that we cannot technically quantify NOP receptor expression levels. The low transfection efficiency precludes us from obtaining detectable protein levels. Nevertheless, our functional assay (e.g., whole-cell patch-clamp) does allow us to measure the basal facilitation ratio that is routinely used as an indicator of tonic G protein modulation of Ca^{2+} channels (Ikeda, 2004). Our results clearly show that when the receptor cDNA concentration microinjected was greater than 100 ng/μl, the mean basal facilitation ratio increased significantly compared with uninjected neurons or those transfected with 10 and 50 ng/μl cDNA. Thus, the enhanced basal facilitation ratio and tonic Ca^{2+} channel inhibition correlated with the higher microinjected cDNA concentrations. The results also demonstrated that the enhanced basal facilitation ratio resulting from NOP receptor overexpression was PTX-sensitive.

The results presented also show that the presence of external Na^+ exerted allosteric effects on the N/OFQ-mediated Ca^{2+} current inhibition in nontransfected SG neurons. However, these effects were unlike most studies that have used NOP receptors (Dooley and Houghten, 2000). With most assays performed in expression systems, the presence of Na^+ has been reported to decrease agonist affinity, shift the agonist potency rightward, decrease receptor binding sites (e.g., B_{max}), and exert variable effects on antagonist properties (Ardati et al., 1997; Butour et al., 1997). Although the N/OFQ efficacy for Ca^{2+} current inhibition remained relatively unchanged, the IC_{50} for both 60 and 120 mM Na^+ decreased compared with the group of neurons in which Na^+ was absent. The results also show that the Hill coefficients were significantly altered by the Na^+ concentrations. The absence of Na^+ resulted in a coefficient value greater than 2.0, whereas it was 0.5 in 120 mM Na^+. Intermediate Hill coefficient values were measured for 12 and 60 mM Na^+. Thus, with minimal changes in potency, the N/OFQ concentration-response curves became steeper as Na^+ was decreased or removed altogether. These data suggest that in our model system, N/OFQ binding to NOP receptors is perturbed in the absence of Na^+, most evident at lower agonist concentrations. The differences observed between our results and those using biochemical assays are probably due to the experimental conditions used. Overall, these findings suggest that under physiological conditions (i.e., >120 mM), Na^+ may effect NOP receptor conformation and increase the binding of N/OFQ without disrupting the coupling with Ca^{2+} channels.

Our results indicate that when NOP receptors were constitutively active, Na^+ exposure rapidly and reversibly removed the tonic Ca^{2+} current inhibition. On the other hand, the three receptor blockers that exerted inverse agonism also removed the tonic current inhibition but nonreversibly. The two-state model is the most commonly used model used to explain the Na^+-mediated allosteric effects. As a result, the role of Na^+ is to stabilize the constitutively active receptor from the active to the resting state (de Ligt et al., 2000; Seifert and Wenzel-Seifert, 2002; Strange, 2002). It is believed that Na^+ binds to an aspartate residue located in the second transmembrane domain that is common to several GPCRs. It is possible that when NOP receptors are constitutively active, the binding site for both Na^+ and blockers is distinct. In a similar fashion, our results also show that constitutively active MOP receptors in SG neurons are allosterically modulated by Na^+ ions, and the blocker CTAP can exert inverse agonism.

It was shown previously that NOP receptor overexpression resulted in tonic inhibition of N-type Ca^{2+} channel currents (Beedle et al., 2004). These findings supported the idea that the tonic NOP receptor-mediated inhibition of Ca^{2+} channels possibly modulates the long-term synaptic depression of pain sensation and contributes to the development of drug tolerance. In support of these studies, we also found that the tonic current inhibition of NOP receptor-transfected neurons was mediated by N-type Ca^{2+} channels because the enhanced basal facilitation ratio was abolished in the presence of ω-conotoxin GVIA. The results of the present study may provide an insight into the mechanisms by which the response to inverse agonists is influenced by NOP receptor activity. Unlike classic opioids, N/OFQ (endogenous or exogenously applied) exerts pronociceptive and antinociceptive effects at supraspinal and spinal sites, respectively (Mogil and Pasternak, 2001; Zeilhofer and Calò, 2003). Furthermore, given that animal pain models (Andoh et al., 1997; Jia et al., 1998; Briscini et al., 2002) and clinical studies (Ko et al., 2002) show increases in N/OFQ or NOP receptor expression, the pharmacological data may help explain why NOP receptor activity (silent or constitutively active) may differentially influence pain processing pathways.

In conclusion, this is the first report demonstrating that constitutively active NOP receptors in SG neurons exhibit differential pharmacology with four high-affinity antagonists (weak partial agonists or inverse agonists). Second, the constitutive activation of NOP receptors was removed in the presence of Na^+ ions or when pretreated with PTX. Finally, the presence of Na^+ ions (60 and 120 mM) resulted in a slight leftward shift of the N/OFQ-mediated Ca^{2+} current inhibition in SG neurons compared with conditions in which Na^+ was absent.

References

Andoh T, Itoh M, and Kuraishi Y (1997) Nociceptin gene expression in rat dorsal root ganglia induced by peripheral inflammation. *Neuroreport* **8:**2793–2796.

Ardati A, Henningsen RA, Higelin J, Reinscheid RK, Civelli O, and Monsma FJ Jr (1997) Interaction of [3H]orphanin FQ and 125I-Tyr14-orphanin FQ with the orphanin FQ receptor: kinetics and modulation by cations and guanine nucleotides. *Mol Pharmacol* **51:**816–824.

Barnes TA, McDonald J, Rowbotham DJ, Duarte TL, and Lambert DG (2007) Effects of receptor density on Nociceptin/OrphaninFQ peptide receptor desensitisation: studies using the ecdysone inducible expression system. *Naunyn Schmiedebergs Arch Pharmacol* **376:**217–225.

Beedle AM, McRory JE, Poirot O, Doering CJ, Altier C, Barrere C, Hamid J, Nargeot J, Bourinet E, and Zamponi GW (2004) Agonist-independent modulation of N-type calcium channels by ORL1 receptors. *Nat Neurosci* **7:**118–125.

Briscini L, Corradini L, Ongini E, and Bertorelli R (2002) Up-regulation of ORL-1 receptors in spinal tissue of allodynic rats after sciatic nerve injury. *Eur J Pharmacol* **447:**59–65.

Butour JL, Moisand C, Mazarguil H, Mollereau C, and Meunier JC (1997) Recognition and activation of the opioid receptor-like ORL 1 receptor by nociceptin, nociceptin analogs and opioids. *Eur J Pharmacol* **321:**97–103.

Calo G, Guerrini R, Rizzi A, Salvadori S, Burmeister M, Kapusta DR, Lambert DG, and Regoli D (2005) UFP-101, a peptide antagonist selective for the nociceptin/orphanin FQ receptor. *CNS Drug Rev* **11:**97–112.

Costa T and Herz A (1989) Antagonists with negative intrinsic activity at delta opioid receptors coupled to GTP-binding proteins. *Proc Natl Acad Sci USA* **86:**7321–7325.

Costa T, Lang J, Gless C, and Herz A (1990) Spontaneous association between opioid receptors and GTP-binding regulatory proteins in native membranes: specific regulation by antagonists and sodium ions. *Mol Pharmacol* **37:**383–394.

De Castro F, Geijo-Barrientos E, and Gallego R (1997) Calcium-activated chloride current in normal mouse sympathetic ganglion cells. *J Physiol* **498:**397–408.

de Ligt RA, Kourounakis AP, and IJzerman AP (2000) Inverse agonism at G protein-

coupled receptors: (patho)physiological relevance and implications for drug discovery. *Br J Pharmacol* **130:**1–12.
Dooley CT and Houghten RA (2000) Orphanin FQ/nociceptin receptor binding studies. *Peptides* **21:**949–960.
Fischetti C, Camarda V, Rizzi A, Pelà M, Trapella C, Guerrini R, McDonald J, Lambert DG, Salvadori S, Regoli D, et al. (2009) Pharmacological characterization of the nociceptin/orphanin FQ receptor non peptide antagonist Compound 24. *Eur J Pharmacol* **614:**50–57.
Fuller BC, Sumner AD, Kutzler MA, and Ruiz-Velasco V (2004) A novel approach employing ultrasound guidance for percutaneous cardiac muscle injection to retrograde label rat stellate ganglion neurons. *Neurosci Lett* **363:**252–256.
Goto Y, Arai-Otsuki S, Tachibana Y, Ichikawa D, Ozaki S, Takahashi H, Iwasawa Y, Okamoto O, Okuda S, Ohta H, et al. (2006) Identification of a novel spiropiperidine opioid receptor-like 1 antagonist class by a focused library approach featuring 3D-pharmacophore similarity. *J Med Chem* **49:**847–849.
Ikeda SR (1991) Double-pulse calcium channel current facilitation in adult rat sympathetic neurones. *J Physiol* **439:**181–214.
Ikeda SR (2004) Expression of G-protein signaling components in adult mammalian neurons by microinjection. *Methods Mol Biol* **259:**167–181.
Jia Y, Linden DR, Serie JR, and Seybold VS (1998) Nociceptin/orphanin FQ binding increases in superficial laminae of the rat spinal cord during persistent peripheral inflammation. *Neurosci Lett* **250:**21–24.
Ko MH, Kim YH, Woo RS, and Kim KW (2002) Quantitative analysis of nociceptin in blood of patients with acute and chronic pain. *Neuroreport* **13:**1631–1633.
Lambert DG (2008) The nociceptin/orphanin FQ receptor: a target with broad therapeutic potential. *Nat Rev Drug Discov* **7:**694–710.
Margas W, Sedeek K, and Ruiz-Velasco V (2008) Coupling specificity of NOP opioid receptors to pertussis-toxin-sensitive Galpha proteins in adult rat stellate ganglion neurons using small interference RNA. *J Neurophysiol* **100:**1420–1432.
Marti M, Stocchi S, Paganini F, Mela F, De Risi C, Calo' G, Guerrini R, Barnes TA, Lambert DG, Beani L, et al. (2003) Pharmacological profiles of presynaptic nociceptin/orphanin FQ receptors modulating 5-hydroxytryptamine and noradrenaline release in the rat neocortex. *Br J Pharmacol* **138:**91–98.
McDonald J, Barnes TA, Okawa H, Williams J, Calo' G, Rowbotham DJ, and Lambert DG (2003) Partial agonist behaviour depends upon the level of nociceptin/orphanin FQ receptor expression: studies using the ecdysone-inducible mammalian expression system. *Br J Pharmacol* **140:**61–70.
Meunier JC, Mollereau C, Toll L, Suaudeau C, Moisand C, Alvinerie P, Butour JL, Guillemot JC, Ferrara P, and Monsarrat B (1995) Isolation and structure of the endogenous agonist of opioid receptor-like ORL1 receptor. *Nature* **377:**532–535.
Mika J, Schäfer MK, Obara I, Weihe E, and Przewlocka B (2004) Morphine and endomorphin-1 differently influence pronociceptin/orphanin FQ system in neuropathic rats. *Pharmacol Biochem Behav* **78:**171–178.
Milligan G and Smith NJ (2007) Allosteric modulation of heterodimeric G-protein-coupled receptors. *Trends Pharmacol Sci* **28:**615–620.
Mogil JS and Pasternak GW (2001) The molecular and behavioral pharmacology of the orphanin FQ/nociceptin peptide and receptor family. *Pharmacol Rev* **53:**381–415.
Olianas MC and Onali P (2003) Sodium ions and GTP decrease the potency of [Nphe1]N/OFQ(1-13)NH2 in blocking nociceptin/orphanin FQ receptors coupled to cyclic AMP in N1E-115 neuroblastoma cells and rat olfactory bulb. *Life Sci* **72:**2905–2914.
Reinscheid RK, Nothacker HP, Bourson A, Ardati A, Henningsen RA, Bunzow JR, Grandy DK, Langen H, Monsma FJ Jr, and Civelli O (1995) Orphanin FQ: a neuropeptide that activates an opioidlike G protein-coupled receptor. *Science* **270:**792–794.
Ruiz-Velasco V, Puhl HL, Fuller BC, and Sumner AD (2005) Modulation of Ca^{2+} channels by opioid receptor-like 1 receptors natively expressed in rat stellate ganglion neurons innervating cardiac muscle. *J Pharmacol Exp Ther* **314:**987–994.
Seifert R and Wenzel-Seifert K (2002) Constitutive activity of G-protein-coupled receptors: cause of disease and common property of wild-type receptors. *Naunyn Schmiedebergs Arch Pharmacol* **366:**381–416.
Shinkai H, Ito T, Iida T, Kitao Y, Yamada H, and Uchida I (2000) 4-Aminoquinolines: novel nociceptin antagonists with analgesic activity. *J Med Chem* **43:**4667–4677.
Strange PG (2002) Mechanisms of inverse agonism at G-protein-coupled receptors. *Trends Pharmacol Sci* **23:**89–95.
Trapella C, Fischetti C, Pela' M, Lazzari I, Guerrini R, Calo' G, Rizzi A, Camarda V, Lambert DG, McDonald J, et al. (2009) Structure-activity studies on the nociceptin/orphanin FQ receptor antagonist 1-benzyl-N-{3-[spiroisobenzofuran-1(3H),4′-piperidin-1-yl]propyl} pyrrolidine-2-carboxamide. *Bioorg Med Chem* **17:**5080–5095.
Trapella C, Guerrini R, Piccagli L, Calo' G, Carra' G, Spagnolo B, Rubini S, Fanton G, Hebbes C, McDonald J, et al. (2006) Identification of an achiral analogue of J-113397 as potent nociceptin/orphanin FQ receptor antagonist. *Bioorg Med Chem* **14:**692–704.
Zaveri N, Jiang F, Olsen C, Polgar W, and Toll L (2005) Small-molecule agonists and antagonists of the opioid receptor-like receptor (ORL1, NOP): ligand-based analysis of structural factors influencing intrinsic activity at NOP. *AAPS J* **7:**E345–E352.
Zeilhofer HU and Calò G (2003) Nociceptin/orphanin FQ and its receptor–potential targets for pain therapy? *J Pharmacol Exp Ther* **306:**423–429.
Zhu Y and Ikeda SR (1993) Anomalous permeation of Na+ through a putative K+ channel in rat superior cervical ganglion neurones. *J Physiol* **468:**441–461.

Address correspondence to: Dr. Victor Ruiz-Velasco, Department of Anesthesiology, Penn State College of Medicine, Hershey, PA 17033-0850. E-mail: vruizvelasco@psu.edu